



## Review of cold spraying and its use for metallic glass coatings

Juan Su, Jia-jie Kang, Wen Yue, Guo-zheng Ma, Zhi-qiang Fu, Li-na Zhu, Ding-shun She, Hai-dou Wang & Cheng-biao Wang

To cite this article: Juan Su, Jia-jie Kang, Wen Yue, Guo-zheng Ma, Zhi-qiang Fu, Li-na Zhu, Ding-shun She, Hai-dou Wang & Cheng-biao Wang (2019) Review of cold spraying and its use for metallic glass coatings, *Materials Science and Technology*, 35:16, 1908-1923, DOI: [10.1080/02670836.2019.1654240](https://doi.org/10.1080/02670836.2019.1654240)

To link to this article: <https://doi.org/10.1080/02670836.2019.1654240>



Published online: 19 Aug 2019.



Submit your article to this journal [↗](#)



Article views: 167




View related articles [↗](#)



View Crossmark data [↗](#)

## Review of cold spraying and its use for metallic glass coatings

Juan Su<sup>a</sup>, Jia-jie Kang <sup>a,b,d</sup>, Wen Yue<sup>a,d</sup>, Guo-zheng Ma<sup>c</sup>, Zhi-qiang Fu<sup>a,d</sup>, Li-na Zhu<sup>a,d</sup>, Ding-shun She<sup>a,d</sup>, Hai-dou Wang<sup>a,c</sup> and Cheng-biao Wang<sup>d,e</sup>

<sup>a</sup>School of Engineering and Technology, China University of Geosciences, Beijing, China; <sup>b</sup>Key Laboratory of Deep GeoDrilling, Technology of Ministry of Natural Resources, Beijing, China; <sup>c</sup>National Key Lab for Remanufacturing, Academy of Armored Forces Engineering, Beijing, People's Republic of China; <sup>d</sup>Zhengzhou Institute, China University of Geosciences, Beijing, Zhengzhou, People's Republic of China; <sup>e</sup>Zhengzhou Institute of Multipurpose Utilization of Mineral Resources, Chinese Academy of Geological Sciences, Zhengzhou, People's Republic of China

### ABSTRACT

Cold spraying (CS), a solid-state spraying technology, is expected to become an appropriate supplementary for traditional spraying methods owing to its plenty of merits such as high deposition efficiency, low temperature and little influence on the particles/substrate. The most reported researches are bulk alloys fabricated by CS. However, the systematic introduction and cold-sprayed metallic glass coatings have not been summarised. Therefore, in this paper, the international research status of CS including equipment structure, spraying process and parameters, advantages and disadvantages, deposit features and bonding mechanism were introduced. By using this technology, the successful researches about Fe-, Al-, Ni-, Cu- and Zr-based amorphous alloy coatings are reported. To overcome the limitations, further development and solutions were proposed.

### ARTICLE HISTORY

Received 6 June 2019  
Revised 5 August 2019  
Accepted 6 August 2019

### KEYWORDS

Cold spraying; deposit mechanisms; spraying parameters; metallic glass coatings; advantages and disadvantages; Reynold number theory; homogeneous and inhomogeneous deformation; Newtonian and non-Newtonian flow

### Introduction





Cold spraying (CS), or cold gas dynamic spraying is a newly developed technology after traditional thermal spraying methods [1–5]. In history, this method dated from a century ago. Thurston first published a patent and demonstrated that metal particles deposited on the metal board at the dragging force of explosive gas or compressed gas in 1902. However, the highest in-flight velocity only reached  $300 \text{ m s}^{-1}$  due to the limitations of technology development. In the 1950s, an innovative design of Laval nozzle made it possible that the particle speed reached supersonic velocity, which pushed the technique achieving tremendous progress. Later on, Soviet scientist A. P. Alkhimov as well as his co-workers studied individual metal particle dragged by the compressed gas flow depositing on various shape surfaces of underlying materials and published two valuable patents in the 1980s. One of the patents introduced this specific method and the other illustrated the equipment which could make the metal powders accelerate with the help of high-pressure gas and undergo plastic deformation on the substrate surfaces obtaining compact and highly bonded coatings. The term of cold gas dynamic spraying was first proposed in a patent issued by A. P. Alkhimov and his colleagues in 1994. For nearly

40 years, CS has efficiently and rapidly developed into a means of deposit method which allowed the deposition of various materials, such as metals, alloys, polymers, noncrystals, nanomaterials and composite materials.

Metallic glasses (MGs), also called amorphous alloys, have short to medium-range atomic configuration which avoids grain boundary or dislocation [6,7]. MGs have a large variety of advantages over the common crystals, such as high strength, unique elongation and ductility, outstanding corrosion resistance and wear resistance. Considering the glass-forming ability (GFA), practical working condition and economic cost, metallic glass coatings (MGCs) have a wide range of applications [8] in the material surface technique area, which are mainly surface functionality for protection or specific physical properties and dimensional restoration for disabled components.

### Introduction of CS system

CS is a means of deposition/consolidation of solid particles in order to fabricate coatings and bulk materials. The structure of CS system is illustrated as Figure 1. The in-flight particles stay in solid state during the spraying process, which differs significantly from the

**CONTACT** Jia-jie Kang  kangjiajie@cugb.edu.cn  School of Engineering and Technology, China University of Geosciences, Beijing 100083, People's Republic of China; Key Laboratory of Deep GeoDrilling, Technology of Ministry of Natural Resources, Beijing 100083, People's Republic of China; Zhengzhou Institute, China University of Geosciences, Beijing 451283, Zhengzhou, People's Republic of China; Guo-zheng Ma  magz0929@163.com  National Key Lab for Remanufacturing, Academy of Armored Forces Engineering, Beijing 100072, People's Republic of China

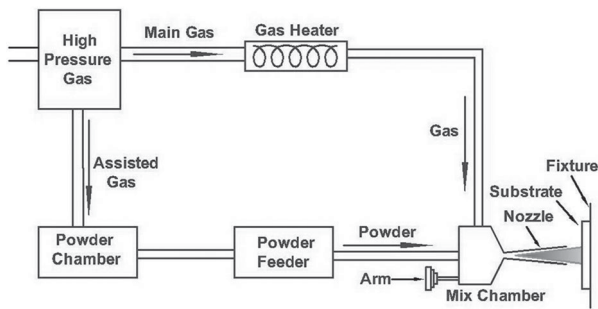


**Figure 1.** Schematic structure of CS system.

conventional thermal spraying methods. High-pressure heated gas flow undergoes converging and diverging when passing through the Laval nozzle and drags the spraying powders ejecting on the substrate surfaces at a sonic velocity. The main gas flow gets to high speed at the effect of high pressure and preheating temperature. Meanwhile, the particles are accelerated to a certain velocity. When the in-flight speed of particles is over the critical velocity, the interface between particles and substrate yields adiabatic shear instability, thus particles undergo severe plastic deformation and deposit on the workpiece surfaces [9–11]. While the deposition mechanism for metallic glass is completely different. Generally, to get higher gas flow speed, the carrier gas is often preheated to reach the temperature range of 40–70% of particle's melting point.

The whole CS system is classified into three parts, including high-pressure gas supply equipment which contains gas heater to push the carrier gas flow, gas and powder control system which connects powder feed chamber and powder gas system, as well as workstation which includes the spraying device and substrate supporting device. The carrier gas used for particle acceleration can be nitrogen, helium, or a mixture of the two, or compressed air. Feed chamber, the pivot of gas flow, powders flow and Laval nozzle, is the main part of the spraying device. The pressure and temperature of carrier gas, the key process parameters, are controlled by a pressure regulator and temperature regulator in the centre control system. The spray gun and substrate support, pulled by the mechanical arm, can stay still or rotate in a certain range according to the spraying requirements. Besides, the substrate is permitted to combine with other multifunctional mechanical equipment to fabricate dimensional free-form materials.

### **Advantages and disadvantages of CS**

Because of low processing temperature, in comparison to the commonly used thermal spray techniques such as high-velocity oxygen fuel spray (HVOF) and laser cladding (LC), particles in CS stay in solid state before impacting with the substrate. Thus CS is able to limit the unfavourable defects that occur in HVOF and LC, like great oxygen content, obvious phase transfer, severe

re-crystallisation and significant residual stress, etc. In specific, the advantages of CS can be sorted into five categories as follows:

- (1) CS is well suitable for the deposition of the temperature-sensitive materials like MGs and nanocrystallines [12,13], the oxygen-sensitive materials like Al, Cu and Ti metals or alloys and the phase transition-sensitive materials like carbide composite materials.
- (2) CS process shows significantly low porosity and high density, i.e. improved DE value at the specific condition of equivalent or less deposition rates, which may help to reduce shrinkage during any subsequent heat treatment.
- (3) CS is able to keep the nozzle clean and eliminate its clogging, without adding extra the second-phase hard particles.
- (4) The coatings exhibit excellent thermal conductivity and electrical conductivity owing to the superior density and lower oxygen content.
- (5) By applying refined spraying gun, nozzle, and spraying distance, CS is permitted to achieve more precise control over the spraying area on the substrate.
- (6) As the working temperature is lower than that of the thermal spraying process, which means there is less heat inputted into the aimed parts and less possibility to undergo high-temperature deformation, thus it enables materials of various categories to combine [14].

Although CS has a variety of advantages over other spraying methods, a few drawbacks in deposition process restrict the further development and wider application in surface technique industries. The limitations and solutions of CS are listed as follows:

- (1) CS is not appropriate for metals that have weak deposition rate in low temperature. As CS technology has a list of attributes such as solid-state deposition, low-temperature deposition, metals, which have good ductility at the range of working temperature, can be well deposited. Nevertheless, nowadays many efforts have been taken to expand the variety of material systems that are suitable to sufficiently deposit by CS method. Meanwhile, the application of high-pressure cold spray equipment and its leader effect in spraying industry can partly weaken this limitation.
- (2) Particles usually suffer highly deforming at the collision moment in CS process, leading to a decrease of ductility. Researchers have found that this phenomenon can be alleviated by appropriately adjusting and controlling the particle size and temperature.
- (3) A few experiments suggest that the deposition efficiency (DE) is quiet low if the hardness of substrate

and powder differ greatly. Therefore, the hardness of the two should be properly matched, so that immersed particles can experience great plastic deformation and create a more mechanical and less metallurgical bond.

- (4) Compared with thermal spray methods, particles in CS process exhibit non-molten state before impacting on the substrate, which makes the combination is more difficult. In order to push in-flight particles and deposit on the surface of aimed parts, the velocity of carrier gas should be higher, thus the total gas consumption of CS is larger than most thermal spray. However, the innovative gas recovery equipment designed by US Army Research Laboratory makes it possible to reuse 80% helium utilised in spraying procedure [15].

### Deposition mechanisms of cold-sprayed MG particles

For cold-sprayed crystalline materials, the deformation mechanisms of particles have been well studied and understood based on computational simulation and experimental studies. Assadi et al. [9] first put forward the bonding theory of localised deformation and adiabatic shear instabilities for particles impacting the metallic surface and presented the critical velocity affecting the high DE by using finite element simulation. So far adiabatic shear instability is the commonly accepted theory for the deposition of crystalline metals in the CS process [16–20], which is based on dislocation models, e.g. Johnson-Cook plasticity model [9,10,21]. Specifically, work hardening and thermal softening of crystalline materials during the impacting process cooperatively lead to the instability. Metallurgical bonding, mechanical interlocking, oxide layer break up, localised melting, diffusion and interface amorphisation are among the variety of mechanisms to explain bonding.

However, the deposition mechanism of cold-sprayed MG particles is not well explained by adiabatic shear instability and many efforts have been taken to the deposition behaviours of MG particles in CS process [22,23]. As the absence of work hardening effect of amorphous materials, the deformation behaviour of MG particles is governed by viscous flow and thus associated with the cooperative movement of atoms, creation and annihilation of free volume rather than multiple slip planes of crystalline metals, proposed by Heno [24]. The viscous flow status is controlled by the viscosity and velocity of particles at impact.

According to the thermal properties of amorphous materials, MGs turn into the supercooled liquid with low viscosity if heated above the glass transform temperature ( $T_g$ ) [11,25–27]. Therefore, MG at temperature above  $T_g$  was modelled as a viscoplastic material and its plasticity depended on Newtonian viscosity of

the liquid following the Vogel-Fulcher-Tamman (VFT) equation. However, when considering the unrealistic deformation caused by the localised shear on conditions of high strain rates and temperature below  $T_g$ , the theory of the non-linear relationship of the MG viscosity vs. shear stress proposed by Concustell et al. [28] is more adoptable. It should be noted that the shear thinning, i.e. non-Newtonian flow, must transfer to Newtonian flow, for achieving the deposition of the cold-sprayed MG particles at the extreme conditions of high strain rates and effective thermal softening.

Using the finite element analysis and viscous flow theory [29,30], Heno et al. [24] pointed out the Reynolds ( $Re$ ) number theory to describe the rheological behaviour of MG particles and explain the relationship with the DE of MGs in CS process. The  $Re$  value is defined by the ratio of the inertial and viscous effects for the impacting particles. The formulation of  $Re$  is as follows:

$$Re = \rho d V_{imp} / \eta$$

where  $\rho$  is the density of particle,  $d$  is the diameter of particle,  $V_{imp}$  is the velocity of particle at impact point and  $\eta$  is the viscosity of MG particle. As the velocity of particles at impact increases and the viscosity of particle at impact decreases when raising the process temperature, different from crystalline materials, the  $Re$  value of MGs deposition is mainly dependent on the temperature. Similar to the critical velocity, there is a  $Re$  threshold value ( $Re_{crit}$ ) that can lead to the remarkable DEs. By using the constitutive model based on the free volume mechanism [31,32] and Von Mises (VM) yield criterion, the deformation behaviour of the impacting particle in supercooled liquid was simulated. It was found that  $Re$  depended on the viscosity and impact velocity of MG particles, while the viscosity was relative to the strain rates and temperature.

Experimentally, the deformation of MG particles at impact is closely relative to the  $Re$  value. The improved deformation behaviour of the impacting particles occurs when increasing the  $Re$  value. Small  $Re$  leads to the undesired effects such as low deformation, particle fracture and high porosity, while MG particles deform homogeneously with the dense structure at large  $Re$ . Moreover, large  $Re$  value provides the possibilities of improvement of DE value, intersplat bonding strength and bonding at the interface with the substrate.

Numerically, at low  $Re$  number, the impact velocity of MG particles causes the VM stress localised at the side edge of contact area. The shear stress leads to remarkable viscoplastic shear in the particle. On the one hand, the energy dissipated by this rapid deformation cannot relocate to the surrounding area in just a few nanoseconds, leading to the rise of the localised temperature and the decrease of the viscosity. Therefore, the plastic shear behaviour expands from the particle/substrate contact area to the particle inside due to

the softening effect of the particle deformation area and the redistribution of stress [33]. On the other hand, the high stress rates corresponding to the plastic shear mean the localised shear thinning. That is the severe impact can produce the strain localisation and the shear band formation. Taking the two aspects above into account, the shear band of the MG materials above  $T_g$  is formed owing to the high impact strain rate, better than the effect of intrinsic stress relaxation rate of the under-cooled liquid. It is worth noting that the mechanism of the shear localisation in the amorphous materials is completely different from that of crystalline solids. The temperature around the contacting surface appears no rise. Instead, the shear band spread to the interior of the MG particles, leading to the possibility of the particle fracture.

At high  $Re$  number, the maximum shear stress is lower than the critic VM stress value at the initial formation stage of shear band. With the increase in the impact  $Re$  value, the plastic deformation behaviour at the edge of MG particles at impact is more homogeneous without the presence of the shear band, which varies from the initial deposition of particles at low  $Re$  number. According to the rheological behaviour of MGs in the supercooled liquid region, the viscosity of the impacting particles is connected with the deposition rate and localised temperature. The relationship of the viscosity vs. time during impact is that the viscosity of MG particle increases suddenly at the initial impact and then drops to a stable level. The abrupt rise of the viscosity, i.e. the strong deformation, is the indication of non-Newtonian behaviour, while the subsequent drop signifies the occurrence of shear thinning in the particle and the stable viscosity means the deformation undergoes in Newtonian flow.

To sum up, the high DE of cold-sprayed metallic glass materials is based on the homogeneous deformation mechanism at the effect of thermal softening. The viscoplastic deformation of the MG particle at impact is caused by non-Newtonian behaviour. Subsequently, the viscous flow of the MG particle is cooperatively promoted by shear thinning and Newtonian flow.

Interestingly, the  $Re_{crit}$  is also related to the mechanical and thermal properties of the substrate materials [34]. In a recent work, Henao et al. [35] studied and simulated the influence of varieties of substrate materials on the deposition behaviour of cold-sprayed MG particles. When  $Re$  values and the hardness of the substrate increase, the flattening of MG particles is promoted, which is attributed to the progressive decrease of the Newtonian viscosity from the edge to the inner part of the MG particles and the drop of stress threshold for viscoplastic flow.

Considering the unfavourable effects of the inhomogeneous flow such as multiple fracture [36], low porosity and low DE and the desirable advantages of homogeneous flow such as good particle flattening,

high coating density and high DE value, the impact conditions for the deposition of MG particles should be precisely controlled to promote the transition from the non-Newtonian deposition to Newtonian deposition. Therefore the impact  $Re$  number must exceed a certain threshold value, which can be identified by the Weissenberg number ( $Wi$ ) based on the properties of the viscous fluids [37]. The Weissenberg number ( $Wi$ ) characterises the relationship between the inherent relaxation properties of a viscous fluid and the rate of deformation to which the viscous fluid is subjected:

$$Wi = \dot{\gamma}\theta$$

$Wi$  is proportional to the shear strain rate ( $\dot{\gamma}$ ) and the characteristic relaxation time ( $\theta$ ) of the MG. When  $Wi \geq 1$ , the deformation mode is obvious inhomogeneous flow, while homogenous flow is expected when  $Wi < 10$ . That is to say, the formation of shear band and the transition from inhomogeneous flow to homogeneous flow can be determined by the criterion of  $Wi$ .

Previous experiments have concluded that this transition takes place at  $Wi \approx 10$ -20. However, studies by Henao et al. [26,38] revealed that the MG particle can undergo inhomogeneous flow and/or present a localised high elastic component because  $Wi$  number is directly related to the shear strain rate and thus concerned with the impact velocity and mechanical properties of the substrate material.

Published researches have reached a consensus suggesting that the formation of jet flow is a consequence of severe plastic deformation of materials flow based on the adiabatic shear instability for cold-sprayed crystalline materials [38]. For crystalline metals, when the impact velocity is higher than the critical velocity, particles experience highly localised plastic deformation at impact onto the substrate due to the high strain rates. Plasticity is mainly governed by the movement of dislocations and the plastic strain energy is dissipated as heat. The shear localisation caused by thermal softening leads to the highly deformed interfacial region of the particle/substrate, which promotes well-bonding.

However, the thermal interaction and rate of cooling of both metallic glass and substrate materials might cause the changes of the deposition behaviour at impact.

The deposition mechanism of the jetting is not well explained in the field of CS – except for a few works [39,40]. Hassani-Gangaraj et al. [39] simulated the bonding behaviour of a Cu particle impacting a Cu substrate at the critical velocity by Lagrangian finite element model and Johnson-Cook constitutive equation. Comparing the material with thermal softening and the material without thermal softening ability, the results indicated that adiabatic softening absolutely can affect the deformation of jet flow, but it was not fundamentally needed for jetting. The simulation of the deformation

and pressure distribution at impact indicated that the contact zone of the particle, flattened from the edge to the inner part, was highly compressed. The decrease of the lateral velocity led to the pressure waves detached from the particle edge. Therefore, materials adjacent to the high-pressure zone and the free surface released the pressure and produced a localised tension, forming a small jet 'lip' as a consequence of the large pressure gradient caused by the zero pressure of the free surface and the high pressure of flattened materials. As the pressure waves and free surface moved in the same direction - the impact direction, the tension produced was very large. It took a long time to get this pressure released and thus caused the acceleration materials in the form of jets. Simultaneously, the pressure waves spread to the top zone of the particle, moved in the opposite direction and got immediately released with high tension. Moreover, the theoretical simulation provided three stage of jetting formation process, including impact-induced shock, shock detachment and jet formation based on pressure release. In addition, they pointed out that it took just 2.5 ns to initiate the jetting 'lip' on the basis of pressure releases, much faster than the time for jet formation based on shear localisation.

Henaoui et al. [40] pointed out that the Re number of spraying condition, cooling rate of the MG particles and thermal-mechanical properties of the substrate can take an essential effect on the jet formation at the interfacial particle/substrate surface. By changing the substrate types and the Re numbers, the experiment results showed that the viscosity of the interfacial regime decreased, then activated the viscous flow and therefore generated the homogeneous deformation at the condition of large Re number, high-hardness and high-diffusivity substrate materials. With the increase in Re number, the softening and flattening phenomena appear more severe and the lateral viscous flow, namely jet-flow deformation in the contact regime is attributed to the high strain rates and low viscosity. As mentioned above, the viscous flow in the interface bonding area is cooperatively generated by shear thinning and the homogeneous deformation. The high-hardness substrate undergo severe deformation due to high strain rate and high stress level and the shear thinning phenomena are caused by the stress localisation, promoting the viscoplastic deformation, intimate particle/substrate contact and DE. However, when the Re number and the hardness of substrate are too high, the jet flow presented at the edge of MG particles at impact experiences fracture and forms small pieces. Because the high strain rates of the substrate materials and the rapid cooling rates of the MG particles lead to the very thin deformation area as a consequence of the drop of particle temperature. The fracture phenomenon was also explained as a consequence of hydrodynamic tension state in the jet flow [39].

Thus, it can be concluded that the formation of jet flow is essentially a stream of viscous flow with low viscosity that undergoes squeeze, deformation and ejection from the particle/substrate interfacial regime.

### Deposition parameters

DE is a vital index to evaluate whether or not the coatings building-up is appropriate and efficient. Generally, DE is affected by plastic deformation which is influenced by the bonding behaviour of particles/substrate, surface morphology and processing operation. To put in a nutshell, the parameters can be divided into three categories—materials characteristics, geometry factors and process parameters. Here, the detailed subcategories of aforementioned parameters affecting DE in CS process will be classified and explained.

#### Materials characteristics

The size, morphology and shape of powders strongly influence the particle deposition behaviour and consequently affect DE in CS during the spraying process. Besides, the properties of substrate materials can affect the strength of bonding behaviour at the interface.

#### Particle size

The early study of the contribution of well-controlled particles size to the optimal critical velocity by Schmidt et al. [41] provided a clear illustration about the relationship the critical velocity, the impact velocity and particles size, as showed in Figure 2. Small particles were able to accelerate to the relatively high speed but were easy to be hampered by the bow shock effect before reaching the substrate. The critical velocity showed a decreasing tendency with the increase of particles size and reached a steady state. Therefore, the optimum size range was where the impact velocity was higher than the critical velocity and particles deposited under the relatively appropriate impact conditions. Besides, particle size also influences the mechanical properties, such as impact toughness and plasticity [42].

#### Particle shape

Song et al. [43] built the computational fluid mechanics model to analysis the influence of shape factor on CS dynamic characteristics. The simulation results indicated that the speed of particles with smaller shape factor were more easily to reach the propellant gas velocity due to the relatively larger specific surface area. Before the shape factor getting to a certain value, particles deposition rate increased with the rise of shape factor. Once it reached the peak point, particle velocity fell to the spherical particle speed. It is worth noting that improving the carrier gas pressure could remarkably enhance the deposition rates of spherical powders and

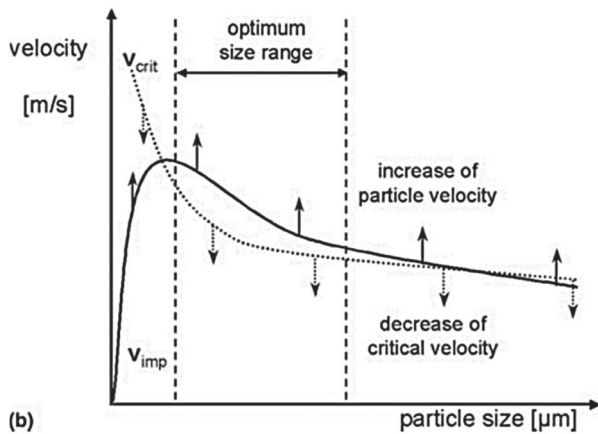


**Figure 2.** Optimisation of particles size range according to the critical velocity and impact velocity [41].

non-spherical powders with larger shape factor. However, the influence caused by changing the gas pressure was negligible for the powders which exhibited little shape factor.

### Substrate roughness

The strength of bonding behaviour is partly influenced by the roughness of substrate materials. The experiment of spraying pure aluminium powders on Al alloy substrate carried by Samson et al. [44] revealed the relationship of increasing the roughness and the coatings bonding strength. Three different coarse surfaces were processed by polishing, shot peening and pulse jetting. The results turned out that increasing the coarse degree of the substrate improved the adhesion strength between the coating and the substrate. Moreover, the residual stress in coatings fabricated by shot peening process or pulse jetting process was unallowable to be neglected, which can produce synergistic effect along with surface morphology and thus enhance the bonding action of coatings.

### Geometric factors

Generally, the geometric effects include spraying standoff distance, spraying angle and nozzle design. The detailed influence is elaborated as follows:

#### Spraying standoff distance

The effect of spraying standoff distance has been investigated by experiments and numerical simulations. A theory has been put forward that there is bow shock wave existing at the gap between spray gun and substrate, which limits the gas velocity and drags particles during the CS process [45]. Pattison et al. [45] pointed out that DE was significantly influenced by the standoff distance due to the bow shock wave and the relative velocity of gas and particles (Figure 3). At the small standoff range, the existence of bow shock limited the deposition behaviour because of the restricted

supersonic potential acceleration distance. At the large standoff range, the shock wave started to disappear. The deposition performance took place positively if the velocity of gas still remained above that of particles. Otherwise, DE dropped down when the gas velocity fell below the particles speed.

### Angles

The influence of spraying angles has been also identified by experiments and numerical investigation.

The numerical analysis conducted by Yin et al. [46] indicated that spraying angle largely influenced the impact velocity and DE. It was found that the impact velocity slightly increased and the strength of bow shock gradually weakened by decreasing the impact angle. Moreover, the growth rate of impact velocity was ascendant with the decline of spraying angle. In a nutshell, DE could fall down when substrate centreline was oblique to the incident direction of particles.

Binder et al. [47] discovered that coatings were highly dense and compact with high bonding microstructure under perpendicular impact conditions. Meanwhile, increasing the deviation from perpendicular impacts always resulted in decreased contact to the substrate surface and DE subsequently. Nevertheless, the result showed that deviations from ideal, perpendicular collision remained in a small range ( $< 20^\circ$ ), thus the deformation characteristics and deposition behaviour of coatings were quite close to ideal specimen, which could be accordant to a large quantity of applicants.

### Design

The nozzle design used in CS affects the powers because the velocity of particles largely depends on the supersonic flow passing through the converging-diverging nozzle [48,49]. In general, there is a maximum Mach number, which is independent of the operating pressure or temperature and is restricted to nozzle geometry. Lee et al. [49] studied the effect of three differential nozzle geometries on flow characteristics. When the Mach number was low, which meant the nozzle was under-expanded, there was high pressure inside the nozzle. Thus the nozzle should have been further expanded in order to restrain the pressure and therefore to enhance the velocity on the outlet. Otherwise, if the nozzle was over-expanded, the pressure inside the nozzle was low, which caused separated or reversed flow inside. Under the circumstance, the nozzle should have been less expanded to avoid ambient air penetrating into the nozzle.

In short, nozzles should be designed to yield a nozzle exit condition that exit pressure is equal to surrounding pressure in order to make up for the loss caused by shock waves and shear interactions. Although operating temperature and pressure both have an influence on

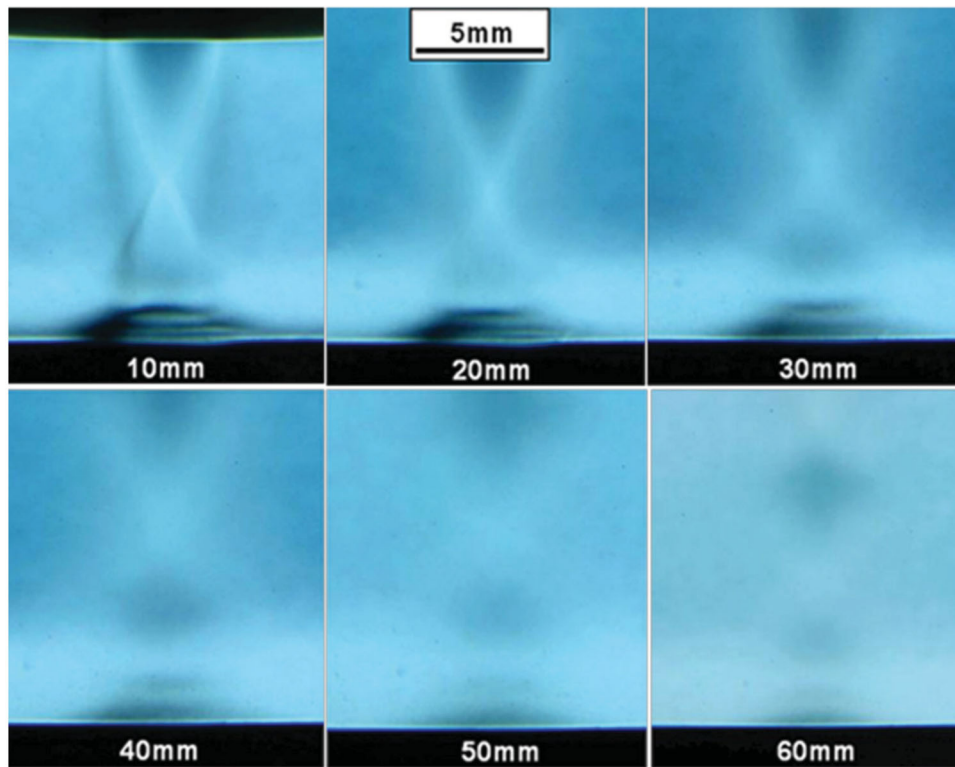


**Figure 3.** Schlieren images of the bow shock at different standoff distances (nitrogen, 30 MPa, 20°C) [45].

the exit pressure it takes fewer effects on the exit pressure by adjusting the temperature. Changing the temperature, on the other hand, is influential in modifying the velocity at the outlet.

### Process parameters

During the spraying process in CS, there is a vital factor - spraying velocity, which decides whether or not coatings deposit on the substrate efficiently. Only the particle velocity reaches the critical velocity are powders capable of forming coatings on the substrate. It is usually considered that the existence of bow shock hampers the flow movement and reduces the particle velocity, and thus hinders the formation of coatings. On the other hand, bow shock can promote gas densification as well as the dragging force, which is in favour of coating formation. The critical velocity mainly depends on carrier gas type, pressure and temperature and relative moving speed of the particle/substrate. Improving all above parameters can increase the particle velocity, meanwhile, particles are more likely to deform and deposit when heating up.

### Gas type

The commonly used carrier gases are nitrogen, argon or both of the two and compressed air. Compared with nitrogen, it has been found that argon has larger viscosity and dynamic output that could drag particles, pointed out in the collected data (Table 1) by Prisco [50]. Besides, the specific heat coefficient is different for various gas types and the coefficient of argon is larger

**Table 1.** Sutherland's constant and reference values for some gases commonly used in CGDS [50].

	C [K]	$T_{ref}$ [K]	$\mu_{ref}$ [ $\mu$ Pa s]
Air	120	291.15	18.27
Nitrogen	111	300.55	17.81
Helium	99	273	19
Argon	135	300	22.9

than that of nitrogen, which means argon has larger velocity leading to the higher speed of dragged particles under the identical nozzle geometry structure and spraying conditions.

### Temperature

Yoon et al. [51] also investigated the effect of gas temperature on the porosity, which is another index related to DE values. The results stated that improving gas temperature can remarkably reduce the porosity of coatings because the supersonic flow in the converging-diverging nozzle led to the acceleration of particles. Meanwhile, particles with thermal energy and kinetic energy impacted on the substrate surface due to the heat exchange between gas flow and particles in the flight. Thus particles could take fully deformation and effectively bond with substrate materials. Moreover, subsequent deposition particles can undergo valid plastic deformation and produce a strong tamping effect on the already deposited particles. Finally, the porosity of coatings decreased and DE value improved. In addition, various temperatures have an influence on the thickness of coatings. The deposition of 304 stainless



steel particles on interstitial-free steel surface was studied by Meng et al. [52]. Increasing gas temperature led to reduce the coating porosity from  $6\% \pm 0.5\%$  at  $450^\circ\text{C}$  to  $2\% \pm 0.3\%$  at  $550^\circ\text{C}$  and enhanced the cohesive strength of the coatings from  $56 \pm 4$  MPa at  $450^\circ\text{C}$  to  $73 \pm 3$  MPa at  $550^\circ\text{C}$ . However, the higher process temperature raised the requirements for the equipment and increased the economic costs. Moreover, if the temperature was too high, powders with low melting point stuck on the inwall and outlet of spraying gun and subsequently DE value fell down.

### Pressure

A study testified the effect of gas temperature and pressure on Al-based amorphous alloy powders depositing on the aluminium alloy, whose conclusion was accordant with aforementioned results. However, it played the secondary effect on improving the kinetic energy. The results showed that DE value was the highest for larger gas pressure and temperature among eight contrast tests. However, Lioma et al. [53] indicated that the effect of increasing the temperature was minimal if the deposition materials contained hard phase. Conversely, rising the temperature played an important role.

## Preparation of metallic glass coatings by CS

### Types of metallic glass

MGs have become the research emphasis among international materials science since the 1990s [7]. In structure, MGs, with the atomic distribution feature of long-range disorder and medium-range order, avoid the existence of lattice defects, such as grain boundary and dislocation. As for crystals, compressive stress redistributes under a press force leading to the uniform deformation because of the existence of defects. Thus MGs, without such defects, undergo localisation shear instability, strain softening and sudden failure under a press force. In component, MGs exhibit a great number of unique traits including multiple constituents, element distribution uniformity, isotropy and no constituent segregation or enrichment. With respect to performance, MGs show high strength, elastic modulus and prevent itself from intercrystalline corrosion and stress cracking, but poor plasticity and high friability

compared with the commonly used crystalline materials. Therefore, MGs along with such unique advantages are widely used in many fields. Currently, the metallic glass coating systems mainly include Fe-based, Al-based, Ni-based, Cu-based as well as part Zr-based. Few differential characteristics and applications of coatings are illustrated as Table 2.

### Metallic glass coatings by CS process

Owing to the solid-deposition and low-temperature feature exhibited in the CS process, amorphous alloy coatings fabricated by this technology can effectively reduce porosity and restrain crystallisation phenomenon, which heavily occurs in thermal spraying. Thus the mechanical performance of coatings such as microhardness, wear resistance, corrosion resistance and others can be greatly improved.

### Fe-based MGCs

Fe-based MGCs, with unique soft magnetic property, wear resistance, corrosion resistance, strong GFA and low economic cost, are reckoned as the most prospective surface protection materials in the field of engineering and environment [54,66–69]. At the first stage, the exploration of Fe-based MGCs was fundamental researches and the amorphisation degree was relatively low. Ajdelsztajn et al. [70] successfully produced Fe–Cr–Mo–W–C–Mn–Si–Zr–B MGCs on the aluminium alloy substrate by CS technology, whose integrity was remarkable; porosity was ultralow along with nominal microcracks. The microhardness value of coating was  $639 \pm 16$  HV<sub>0.3</sub>, about 12-fold over the substrate. However, the amorphisation degree was mediocre as a part of particles were not completely amorphous. The thickness of coating was only approximately 0.2 mm, which may not meet the complex conditions such as long-term service or corrosive environment. At the interface of coating/substrate, it was observed that the undeformed particles embedding into substrate body as showed in Figure 4 and this phenomenon paved the path for hard particles embedding, depositing and forming hard coatings on the soft substrate, while some weak bonds and fractures influenced the adhesion strength of coating/substrate. Afterwards

**Table 2.** Features and application of several systems.

System	Features	Application	Ref.
Fe-based	Enhanced hardness, high crystallisation temperature, excellent corrosion and wear resistance, strong glass forming ability, low cost	Hydraulic machinery, power plants, coastal installations	[54–57]
Al-based	High strength to weight ratio, strong corrosion resistance, densified structure	Aircraft and automobile industries, Environment protections, sacrifice anode protection	[58–60]
Ni-based	Ultrahigh strength, high thermal stability, excellent corrosion resistance, high process cost	Fuel cell environments, glass industries, nuclear fuel reprocessing	[61,62]
Cu-based	Good nanoscale wear resistance, unique mechanical property	Micro-electro-mechanical devices, turbine blades	[63]
Zr-based	High fracture toughness, unique ductility, high hardness and density, ultrahigh corrosion resistance	Nuclear waste retexture equipment, repair or replacement of body tissue, bearings	[64,65]

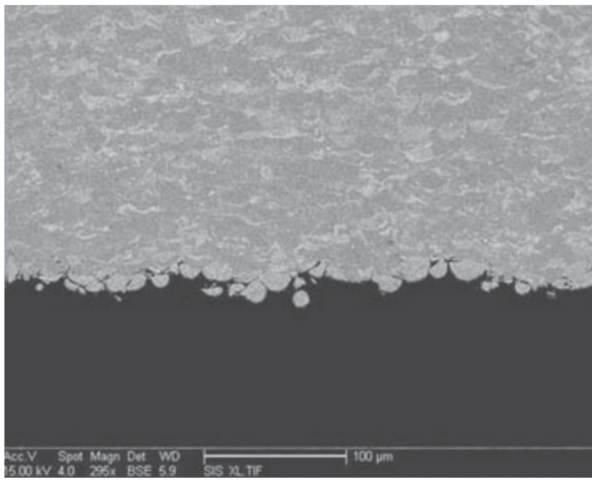


**Figure 4.** Backscattered electron image of the interface between the coating and the substrate [70].

several researches of CS Fe-based MGCs were carried on. The performance parameters such as component, porosity, DE as well as hardness are summarised in Table 3.

With the improvement of technology and the expansion of coatings in the industry protection field, researchers took a forward step to test the wear resistance and corrosion resistance of Fe-based MGCs. Yoon et al. [73] prepared  $\text{Fe}_{68.8}\text{C}_{7.0}\text{Si}_{3.5}\text{B}_{5.0}\text{P}_{9.6}\text{Cr}_{2.1}\text{Mo}_{2.0}\text{Al}_{2.0}$  (at.-%) coating on the surface of low-carbon steel. The average microhardness of the coating reached 820  $\text{HV}_{0.1}$ , which was remarkably higher than that of general bearing steel and SBS bearing sample. With respect to the tribology behaviour by the pin-on-disc method at room temperature, the friction coefficient of the experimental sample was lower than that of general bearing steels and higher than that of SBS bearing. Figure 5 shows weight loss and the morphology of the tracks. It is found that coating surface experienced strong plastic deformation together with grooves and debris and no obvious cracks, which manifested that the main wear mechanism were abrasive wear and adhesive wear. The result also turned out that cold-sprayed coating exhibited better tribology performance than thermal sprayed ones. With the unique hardness and wear resistance [74,75], Fe-based MGCs exhibit similarities with polycrystalline Diamond [76].

With regard to the corrosion behaviour of Fe-based MGCs, Choi et al. [77] fabricated  $\text{Fe}_{68.6}\text{C}_{7.1}\text{Si}_{3.3}\text{B}_{5.5}\text{P}_{8.7}\text{Cr}_{2.3}\text{Al}_{2.0}\text{Mo}_{2.5}$  (at.-%) coatings by plasma thermal spraying and CS and discussed the corrosion mechanism in 3.5 wt-% NaCl solution. Compared with

thermal spray coatings, the high pitting potentials of cold spray coatings in potentiodynamic polarisation curves indicated highly localised corrosion potential (Figure 6). Generally accepted corrosion mechanism is that corrosion behaviour often initiates in pore surfaces and inter-splat boundaries where chemical component and phase structure distribution are heterogeneous. Owing to the low-temperature feature, the proportion of amorphous phase in cold spray coating was higher and the micro-defects and grain boundaries, acting as the potential nucleation sites, were largely decreased causing the corrosion current shrank. Moreover, the corrosion test of partial crystallisation, whole amorphisation and whole crystallisation further testified micro-pores and amorphisation degree.

### Al-based MGCs

With the lightweight tendency of aerospace and transportation, the demand for low-density, high-strength materials are increasingly putting on the agenda and getting much attention from the scientific community. Al-based MGCs, a nascent material system as a substitute of commonly used Al-alloys, exhibit high strength to weight ratio, low density, low-temperature deposition as well as improved wear and corrosion resistance. Unfortunately, the general deficiency of Al-based MGCs is relatively low GFA and likely to be oxidised by oxygen in the atmosphere. To date, many achievements have been made to enhance the performance of Al-based MGCs in various aspects.

Then many efforts have been taken to explore the composition design because of the ability of glass formation and the influence of phase structure. Generally, the systems of Al-based MGCs contain of ternary elements in the form like Al-TM-RE, where TM is a transition element (i.g. Ni, Co or Fe) coupled with the function of accelerating the atomic packing procession while RE is a rare earth element (i.g. La, Ce, Gd or Y) in order to contribute to glass formation. As respect to the cold-sprayed Al-based system, it includes Al-Co-Ce [60,78] Al-Ni-Ce [79], Al-Y-Ni-Co-Sc [80], Al-Ni-Y-Co-La [81].

Like the research development of Fe-based MGCs, the studies of Al-based MGCs began from the composition design and structure characterisation, such as the amorphous fraction, porosity and hardness, then came to the performance test like wear and corrosion behaviour. After the first study of the localised corrosion behaviour by adjusting component with the amorphous Al-Co-Ce system [60], the system of Al-Ni-Ce

**Table 3.** Performance parameters of Fe-based amorphous alloy coatings prepared by CS.

Year	Materials system	Porosity	DE	Amorphous degree	Microhardness	Ref.
2009	$\text{Fe}_{73.5}\text{Cu}_1\text{Nb}_3\text{Si}_{13.5}\text{B}_9$	–	–	–	–	[71]
2012	$\text{Fe}_{44}\text{Co}_6\text{Cr}_{15}\text{Mo}_{14}\text{C}_{15}\text{B}_6$	2.5%	> 70%	> 98%	1100 $\text{HV}_{0.3}$	[43]
2015	$\text{Fe}_{73}\text{Cr}_2\text{Si}_{11}\text{B}_{11}\text{C}_3$	< 0.5%	84%	–	820 $\text{HV}_{0.3}$	[28,72]

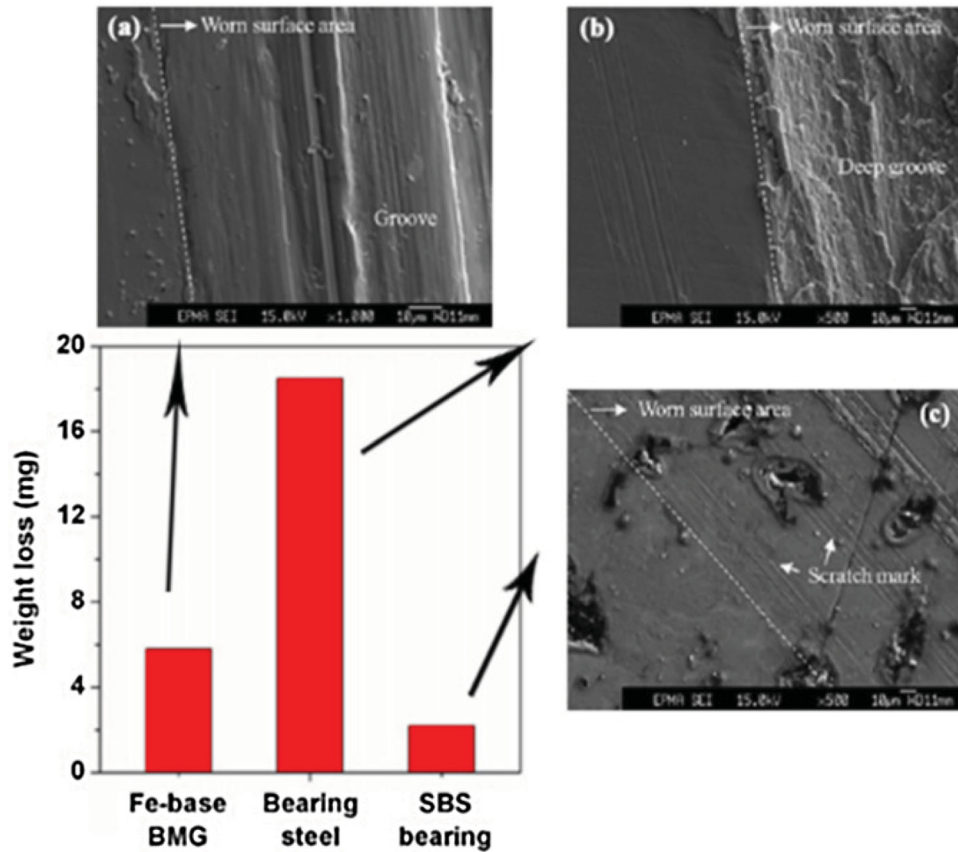


Figure 5. Weight loss, and appending morphology of (a) Fe-based BMG, (b) bearing steel and (c) SBS bearing [73].

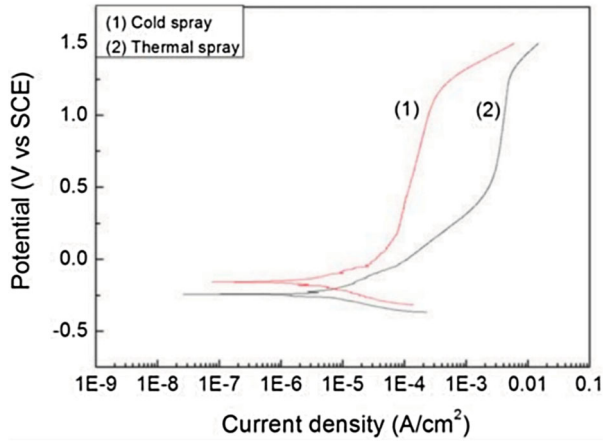


Figure 6. The potentiodynamic polarisation curves of coatings in the 3.5% NaCl solution [77].

amorphous alloys powders were sprayed under the gas pressure of 17 bars and the gas temperature of 450°C [79]. The microhardness of MGCs was  $300 \pm 20 \text{ HV}_{0.1}$ , which was higher than that of the conventional Al alloys. At the same time, the tensile bond strength,  $24 \pm 5 \text{ MPa}$ , was stronger than that of Al6061 cold-sprayed coatings under the coincident test. The results of XRD analysis implied that the phase structure and amorphous nature between sprayed coatings and raw powders had little variation, indicating the cold spray technology did not neither input much thermal energy

to coatings nor influence the characteristic of coatings. However, the results of XRD patterns were not very optimistic as few crystal peaks existed and the amorphous fraction was not obvious. Additionally, cold-sprayed Al-Ni-Ce MGCs appeared effectively resistant to chlorine ions invasion and protect the substrate from corrosion.

To keep Al6061 alloys from wear and corrosion, Lahiri et al. [80] synthesised  $\text{Al}_{90.05}\text{Y}_{4.4}\text{Ni}_{4.3}\text{Co}_{0.9}\text{Sc}_{0.35}$  MGCs using CS technology and improved the wear and corrosion resistance. By adopting appropriate spraying conditions of 400°C preheated nitrogen and 3.8 MPa pressure, the coating obtained a dense-packed structure with the porosity of 2%, but the glassy degree did not appear to be impressive as few broad Al-FCC peaks existed. The morphology of sprayed coatings indicated that particles undergone complete deformation and bonded well. Moreover, the high magnification micrograph of coating revealed the flattening and elongation of particles forming splat structure, and depending on empirical relationship for making sure of the plastic strain of the starting powders proposed by Papyrin, the strain turned out to be around 0.57, which meant a significant amount of plastic deformation in virtue of a few proportion of crystalline part. Combining with XRD patterns, differential scanning calorimeter (DSC) plot along with two crystallisation peaks indicated that amorphous component took the prominent part in

sprayed coatings. As for the tribological performance, Al-based MGCs showed 600% improvement of wear resistance whose worn surface was much smoother and free of plowing and cracks compared with the substrate that suffered severe damage and plowing was obviously observed. Besides, potentiodynamic tests of Al-based MGCs in various NaCl concentration showed 5 times corrosion resistance than the substrate owing to the amorphous characteristics and the formation of passive oxide layer  $\text{Al}_2\text{O}_3$ .

As mentioned above, the wear and corrosion performance of MGCs largely depends on the amorphous phase percentage. Therefore, Henao et al. [81] made great efforts to decrease the porosity and the crystalline volume fractions in order to enlarge the space of tribology and corrosion resistance. By adjusting the spraying parameters, the thickness, porosity and hardness of coatings were positively related to gas temperature, gas pressure and standoff distance because higher deformation of the impacting particles resulted in better interparticle bonding and porosity collapse under the tamping effect. The percentages of amorphous phase reached 81%. With regard to the wear performance, the worn loss of Al-based MGCs was less than that of Al-alloy substrate on the normal load and increased when the load added. Interestingly, coefficient of friction (COF) of coatings applied various loads exhibited the identical rapid raise to the top in the initial running-up period because of the presence of a high mean contact pressure during the beginning stage of sliding. With the phenomenon that more extensive abrasive grooving occurs and the amount of particle debris augmented when normal load increased, it was obviously clarified that wear mechanism of Al-based MGCs was abrasive grooving alongside with small fraction of surface splat delamination. As temperature is an essential and sensitive factor to MGCs, especially flash temperature which represents the local surface temperature at contacting asperities exceeding both average surface temperature and surrounding temperature, it should be considered whether flash temperature influenced the sliding results. From the high plastic deformation and oxidation analysed on the wear tracks, it indicated the existence of localised flash temperatures. However, no signs of adhesive waves and molten zones were founded suggesting that flash temperature or average surface temperature had little influence to sliding contact surface. From the potentiodynamic polarisation results, the initiative potential for passive region and transpassive dissolution of Al-based MGCs was higher than that of Al alloys substrate. Moreover, the change of current density between positive and negative scans was much bound up with the stability of the formed passive film, which meant if hysteresis loop was smaller the stability of passive film was better. In fact, the passivation layer stability of MGCs was much excellent than that of alloys as the hysteresis loop was minor.

### **Ni-based MGCs**

In respect of Ni-based MGCs, the research group led by Sanghoon Yoon had a number of publications about NiTiZrSiSn MGCs depending on CS process [27,82–85]. Compared with spraying methods such as vacuum plasma spraying and high-velocity oxyfuel (HVOF) spraying, the advantages of CS technology including less heat input is used to analyse amorphous phase evolution and oxidation behaviour of coatings [82]. The effect of thermal energy and kinetic energy was considered as the internal and significant factor. The degree of amorphous phase transformation and oxidation in CS process was lower than that in HVOF spraying.

Furthermore, they studied how process gas types and additional powder heating influenced the coatings characteristic and individual particle deformation performance [27,83]. By changing the propellant gas type from nitrogen to helium can markedly improve DE value, in accordance with the aforementioned conclusion. Interestingly, splats were formed when particles impacted the substrate and released the energy during the severe localised deformation. With higher dragging force of helium and larger additional powder heating, the ratio of splat to crater was increased and the mechanical properties including bond strength and microhardness were improved.

The tests of tribological behaviour and corrosion performance of Ni-based MGCs were carried out. Compared with partially crystallised samples and fully crystallised samples, amorphous alloy coatings indicated better wear resistance with lower scratch friction coefficient and worn-out cross-sectional area at the applied normal loads ranging from 10 to 190 N [83,84]. After scratched at the normal load, the worn surface of amorphous coatings contained groove with transverse cracks and deformed material pile-up along the path borderline. That indicated Ni-based MGCs possessed both ductile and brittle characteristic features during the wear test attributing to the non-uniform distribution of contact pressure and inherently low ductility of the metallic glass. For the partially crystallised samples, the deformed pile-up phenomenon was severe and the dropped particles acted as grains and caused obvious furrows. On the other hand, severe fracture and spallation were observed for fully crystallised coating as both the fracture strength and fracture strain descended after crystallisation for amorphous materials. In conclusion, amorphous coatings showed better wear resistance than either partially crystallised ones or fully crystallised ones. Wang et al. [85] compared the corrosion behaviour of  $\text{Ni}_{59}\text{Zr}_{20}\text{Ti}_{16}\text{Si}_2\text{Sn}_3$  and  $\text{Ni}_{53}\text{Nb}_{20}\text{Ti}_{10}\text{Zr}_8\text{Co}_6\text{Cu}_3$  obtained by HVOF technology and fully amorphous  $\text{Ni}_{53}\text{Nb}_{20}\text{Ti}_{10}\text{Zr}_8\text{Co}_6\text{Cu}_3$  sprayed by CS method. It was showed that fully amorphous alloy coatings deposited by CS technology had

an inferior corrosion resistance than those of partially MGCs.

### Cu-based MGCs

Except the studies of Ni-based MGCs, the group including Sanghoon Yoon [13] further investigated CuNiTiZr bulk metallic glass coating, more narrowly, the strain-enhanced nanocrystallisation of this kind of amorphous coatings. By increasing the gas pressure and the resultant in-flight particle velocity, the amorphous hump shrank gradually and the enthalpy during the exothermic reaction calculated from heat flow as function of temperature declined slightly, indicating the increase of fraction of crystallisation. Except for the study of low-velocity sprayed coatings, individual particles underwent severe plastic deformation under high strain rate and high gas speed. The increase of the particle impact speed led to produce higher strain and heat energy that dispersed at a larger area of amorphous phase and the resultant enhanced crystallisation degree.

To limit the nucleation kinetics for the under-cooled liquid and consequent less crystallisation degree, it is important to widen the process regimes for lower cooling rates. For the past few decades, specialists discovered several disciplines about how to design the alloy components, including the types of element, amount of components and size differences among atoms, to decrease nucleation kinetics and thus improve the GFA. One of the most classical and adopted empirical laws was to design three or even more components of amorphous alloys. Then great efforts were spent to develop new multiple component system. However, despite the common metallic glass systems along with multiple components, binary and ternary component could also form amorphous alloys, such as  $\text{Cu}_{50}\text{Zr}_{50}$  [86] and  $\text{Cu}_{50}\text{Ti}_{20}\text{Ni}_{30}$  [87].

List et al. [86] studied the deformation behaviour of single particles and sequent coating formation with component of amorphous  $\text{Cu}_{50}\text{Zr}_{50}$  by varying the CS process parameters to discover the appropriate deposit conditions. Besides, the relationship between deposition behaviour and impact temperature was calculated and illustrated. The rise of gas temperature was able to directly transfer into a higher particle impact velocity. With different deposit conditions, the single impact morphology could be classified into four categories, which were no bonding, weak bonding, good bonding and viscous flow. It was considered that the former two had less possibility to form coatings well because of the insufficient deformation while the latter two were expected to contribute cold-sprayed valid deposition. This was testified that well-bonded particles were much more remained than other bonding type particles after suffering cavitation attack. As for the coatings properties, the hardness of coatings deposited at 800°C gas temperature was 30% higher than that of coatings

sprayed at 600°C, while the cohesive strength of the former was as half as the latter. The author also pointed out that the cost of depositing MGCs or parts was likely 2–5 less than that of bulk MGCs.

Besides the various applications in the engineering industry, Cu-based MGCs can also function as biomedical materials, such as antibacterial protective coatings taking advantage of unique corrosion resistance [87]. El-Eskandrany and Al-Azmi utilised metallic glassy  $\text{Cu}_{50}\text{Ti}_{20}\text{Ni}_{30}$  which employed as feedstock materials to prepare antibacterial coating on the surface of SUS 304 substrate by CS process [87]. Using the nanoindentation test with a load of 400 mN, metallic glassy  $\text{Cu}_{50}\text{Ti}_{20}\text{Ni}_{30}$  coating possessed extraordinary high-hardness value about  $3.1 \pm 0.1$  GPa and the value of Young's modulus varied between 97 GPa and 111 GPa, which suggested the uniformity and homogeneity in structure and elemental composition of the cold-sprayed  $\text{Cu}_{50}\text{Ti}_{20}\text{Ni}_{30}$  MGCs. Moreover, the COF value of  $\text{Cu}_{50}\text{Ti}_{20}\text{Ni}_{30}$  MGCs was 0.45, much lower than that of the substrate around 0.83. Especially, the microbiological testing studied the inhibitory effect of coated substrate against *E. coli* biofilm formation incubated for different times. The substrate coated with  $\text{Cu}_{50}\text{Ti}_{20}\text{Ni}_{30}$  MGCs remarkably and effectively inhibited colony formation of *E. coli*. Furthermore, the existence of certain amount of Cu and Ti enhanced the antimicrobial effect of Ni. Therefore, it provided a viable possibility and promising future to inhibit colony formation by coating with  $\text{Cu}_{50}\text{Ti}_{20}\text{Ni}_{30}$  MGCs.

### Zr-based MGCs

As for Zr-based metallic glass alloys, bulk ones had been paid more attention than coatings in plenty of researches owing to its unique biocompatibility and practicability in biomedical application [88,89]. Up to now, a large proportion of Zr-based MGCs was produced by copper mould casting [88,90,91], very little was obtained though CS technology. However, Kang et al. [92] added 5% weight fraction of ZrCuAlNiTi MG powders, which were functioned as reinforcement particles, into copper matrix and subsequently fabricate ZrCuAlNiTi/Cu composite coating. The microstructure showed that reinforcements spread relatively evenly and reduced the porosity of deposits, lower than 0.1%. But little interaction between reinforcement particles and the matrix resulted in relatively weak bond strength. Comparing the XRD patterns between mixed powders and as-sprayed composite coatings that were suffered heat treatment at 200, 300 and 500°C, it shows that the phase of ZrCuAlNiTi/Cu composite coating perserved amorphous whether at the CS condition or suffering heat treating below 300°C. The relationship between microhardness and heat treatment temperature of Zr-based MG particles expressed that particles microhardness remained constant about 500 HV when the temperature was below

400°C, while there was sharp increase from 500 HV to 620 HV at 450°C attributed to the recovery of shear bands and crystallisation.

As is known, it could enhance the bonding strength between pure copper particles through the hammering effect by adding a proportion of ZrCuAlNiTi MG powders. Moreover, the mechanical strength including tensile strength, yield strength and Young's modulus of composite coating with metallic glass particles added were better than that of pure copper coating because it was able to enhance the density of dislocation following the strength improved. Then the results of friction tests indicated that ZrCuAlNiTi/Cu composite coating presented less COF and wear rates than whether pure copper coating or composite coating annealing at 300°C, which meant higher wear resistance. Besides, ZrCuAlNiTi MG appeared lower wear rate than conventional ceramic reinforced cold-sprayed composite like Al<sub>2</sub>O<sub>3</sub>. The worn surface analysis showed that the addition of MG particles shrank the contact area between the copper surface and counterpart and restrained the deformation of the composite.

## Conclusion and outlooks

CS has a large potential in fabricating various types of MGCs. It is expected to become a supplementary production technology to thermal spraying attributing to its low energy consumption, no oxidation or phase transformation. Adiabatic shear instability, an existing and developing bonding theory of CS, is mostly accepted by researchers via metallurgical bonding and mechanical bonding. Adjusting appropriate deposition parameters (including geometric factors, materials characteristics and processing parameters) is a significant aspect for good quality of coatings. With a further study of amorphous alloy coatings and the advancement of CS equipment, an increasing number of cold-sprayed MGCs (including Fe-based, Al-based, Ni-based, Cu-based, Zr-based, etc.) is getting more attention. While CS technology has obtained much success both in R&D test and commercial productions, there is still some limitations of CS system, spraying process and MGCs, including:

- (1) With the larger dragging force ability than nitrogen used, helium is often utilised as propulsion gas. Meanwhile, it is expensive due to its scarcity and technical difficulties of recycled utilisation. Therefore, it should be put on agenda that designing a high-efficient and commercialised gas–solid separation and recycling device.
- (2) The fixture of most CS devices stays static or rotates around a central axis but the operating spray gun is fixed resulting in the waste of materials and single function. Thus, the combination of CS with other multifunctional mechanical equipment to fabricate multi-dimensional free-form materials.
- (3) The bonding mechanism for cold-sprayed MG materials is not based on adiabatic shear instabilities, but is closely related to *Re* value at impact, which is influenced by the impact velocity and the flow viscosity. The high DE is based on the homogeneous deformation mechanism and the viscous flow of the MG particle is cooperatively promoted by shear thinning and Newtonian flow.
- (4) It is really hard to obtain complete amorphous MGs. Therefore, too many efforts should be taken to improve the amorphisation degree of existing amorphous materials. Moreover, exploring new material systems or new types of components with higher MGF is necessary to meet various needs.
- (5) As demonstrated before, the porosity of coatings is directly related to the quality when served in a different environment. The less porosity is, the better performance will be.
- (6) The performance testing of Fe-based, Al-based, Ni-based, Cu-based, Zr-based MGCs is not systematic. Besides, there is no standard to judge the feasibility of coatings. The comprehensive properties, such as wear tests and corrosion tests, should be simulated under actual working conditions where materials practically served.

## Funding

This work was supported by the National Natural Science Foundation of China: [grant number 41772389]; National Natural Science Foundation of China: [grant number 41872183]; Joint Fund of Ministry of Education for Pre-research of Equipment for Young Personnel Project: [grant number 6141A02033120]; the Pre-Research Program in National 13th Five-Year Plan: [grant number 61409230603]; and National Key Technologies R&D Program of China: [grant number 2018YFC0603403].

## ORCID

Jia-jie Kang  <http://orcid.org/0000-0002-8873-3684>

## References

- [1] Moridi A, Hassani-Gangaraj SM, Guagliano M, et al. Cold spray coating: review of material systems and future perspectives. *Surf Eng.* 2014;30:369–395.
- [2] Rokni MR, Nutt SR, Widener CA, et al. Review of relationship between particle deformation, coating microstructure, and properties in high-pressure cold spray. *J Therm Spray Techn.* 2017;26(6):1308–1355.
- [3] Li W, Yang K, Yin S, et al. Solid-state additive manufacturing and repairing by cold spraying: a review. *J Mater Sci Technol.* 2018;34(3):440–457.
- [4] Champagne V, Helfritsch D. The unique abilities of cold spray deposition. *Int Mater Rev.* 2016;61(7):437–455.
- [5] Raelison RN, Verdy C, Liao H. Cold gas dynamic spray additive manufacturing today: Deposit possibilities, technological solutions and viable applications. *Mater Design.* 2017;133:266–287.

- [6] Qiao JW. In-situ Dendrite/Metallic Glass Matrix Composites: A review. *J Mater Sci Technol.* 2018;29(8):685–701.
- [7] Kruzic JJ. Bulk metallic glasses as structural materials: A review. *Adv Eng Mater.* 2016;18(8):1308–1331.
- [8] Khan MM, Nemati A, Rahman ZU, et al. Recent advancements in bulk metallic glasses and their applications: A review. *Crit Rev Solid State.* 2017;43(3):233–268.
- [9] Assadi H, Gartner F, Stoltenhoff T, et al. Bonding mechanism in cold gas spraying. *Acta Mater.* 2003;51(15):4379–4394.
- [10] Grujicic M, Zhao CL, DeRosset WS, et al. Adiabatic shear instability based mechanism for particles/substrate bonding in the cold-gas dynamic-spray process. *Mater Design.* 2004;25(8):681–688.
- [11] List A, Gaertner F, Schmidt T, et al. Impact conditions for cold spraying of hard metallic glasses. *J Therm Spray Technol.* 2012;21(3–4):531–540.
- [12] Tailleart NR, Gauthier B, Eidelman S, et al. Metallurgical and physical factors controlling the multi-functional corrosion properties of pulsed thermal-sprayed Al-Co-Ce coatings. *Corrosion.* 2012;68(3):035006.
- [13] Yoon S, Bae G, Xiong Y, et al. Strain-enhanced nanocrystallization of a CuNiTiZr bulk metallic glass coating by a kinetic spraying process. *Acta Mater.* 2009;57(20):6191–6199.
- [14] Yin S, Cavaliere P, Aldwell B, et al. Cold spray additive manufacturing and repair: Fundamentals and applications. *Addit Manuf.* 2018;21:628–650.
- [15] Pattison J, Celotto S, Morgan R, et al. Cold gas dynamic manufacturing: A non-thermal approach to freeform fabrication. *Int J Mach Tool Manu.* 2007;47(3–4):627–634.
- [16] Zhu L, Jen TC, Pan YT, et al. Particle bonding mechanism in cold gas dynamic spray: A three-dimensional approach. *J Therm Spray Technol.* 2017;26(8):1859–1873.
- [17] Bielousova O, Kocimski J, Maev RG, et al. Localisation of deformation in cold gas dynamic spraying. *Surf Eng.* 2016;32(9):655–662.
- [18] Meng F, Aydin H, Yue S, et al. The effects of contact conditions on the onset of shear instability in cold-spray. *J Therm Spray Technol.* 2015;24(4):711–719.
- [19] Saleh M, Luzin V, Spencer K. Analysis of the residual stress and bonding mechanism in the cold spray technique using experimental and numerical methods. *Surf Coat Tech.* 2014;252:15–28.
- [20] Walker M. Microstructure and bonding mechanisms in cold spray coatings. *Mater Sci Tech.* 2018;34(17):2057–2077.
- [21] Johnson GR, Cook WH. Fracture characteristics of three metals subjected to various strains, strain rates, temperatures and pressures. *Eng Fract Mech.* 1985;21(1):31–48.
- [22] Hufnagel TC, Schuh CA, Falk ML. Deformation of metallic glasses: Recent developments in theory, simulations, and experiments. *Acta Mater.* 2016;109:375–393.
- [23] Johnson WL, Lu J, Demetriou MD. Deformation and flow in bulk metallic glasses and deeply undercooled glass forming liquids – a self consistent dynamic free volume model. *Intermetallics.* 2002;10(11–12):1039–1046.
- [24] Henao J, Concustell A, Dosta S, et al. Deposition mechanisms of metallic glass particles by Cold Gas Spraying. *Acta Mater.* 2017;125:327–339.
- [25] Zhou X, Wu X, Mou S, et al. Simulation of deposition behavior of bulk amorphous particles in cold spraying. *Mater. Trans.* 2010;51(10):1977–1980.
- [26] Yoon S, Lee C, Choi H, et al. Impacting behavior of bulk metallic glass powder at an abnormally high strain rate during kinetic spraying. *Mater Sci Eng.* 2007;449:911–915.
- [27] Yoon S, Lee C, Choi H, et al. Kinetic spraying deposition behavior of bulk amorphous NiTiZrSiSn feedstock. *Mat Sci Eng A-Struct.* 2006;415(1–2):45–52.
- [28] Concustell A, Henao J, Dosta S, et al. On the formation of metallic glass coatings by means of cold gas spray technology. *J Alloys Compd.* 2015;651:764–772.
- [29] Spaepen F. Homogeneous flow of metallic glasses: A free volume perspective. *Scripta Mater.* 2006;54(3):363–367.
- [30] Bletry M, Guyot P, Brechet Y, et al. Homogeneous deformation of Zr–Ti–Al–Cu–Ni bulk metallic glasses. *Intermetallics.* 2004;12(10–11):1051–1055.
- [31] Jun HJ, Lee KS, Yoon SC, et al. Finite-element analysis for high-temperature deformation of bulk metallic glasses in a supercooled liquid region based on the free volume constitutive model. *Acta Mater.* 2010;58(12):4267–4280.
- [32] Henann D, Anand L. A constitutive theory for the mechanical response of amorphous metals at high temperatures spanning the glass transition temperature: Application to microscale thermoplastic forming. *Acta Mater.* 2008;56(13):3290–3305.
- [33] Pan J, Wang YX, Guo Q, et al. Extreme rejuvenation and softening in a bulk metallic glass. *Nat Commun.* 2018;9(1):560.
- [34] Arabgol Z, Villa Vidaller M, Assadi H, et al. Influence of thermal properties and temperature of substrate on the quality of cold-sprayed deposits. *Acta Mater.* 2017;127:287–301.
- [35] Henao J, Bolelli G, Concustell A, et al. Deposition behavior of cold-sprayed metallic glass particles onto different substrates. *Surf Coat Tech.* 2018;349:13–23.
- [36] Umeda T, Mimura K. Numerical analysis of the impact fracture of metallic glass based on free volume model. *Key Engineering Materials.* 2019;794:188–193.
- [37] Sun YH, Concustell A, Carpenter MA, et al. Flow-induced elastic anisotropy of metallic glasses. *Acta Mater.* 2016;112:132–140.
- [38] Kim K, Watanabe M, Kuroda S. Bonding mechanisms of thermally softened metallic powder particles and substrates impacted at high velocity. *Surf Coat Tech.* 2010;204(14):2175–2180.
- [39] Hassani-Gangaraj M, Veysset D, Champagne VK, et al. Adiabatic shear instability is not necessary for adhesion in cold spray. *Acta Mater.* 2018;158:430–439.
- [40] Henao J, Concustell A, Dosta S, et al. Influence of the substrate on the formation of metallic glass coatings by cold gas spraying. *J Therm Spray Techn.* 2016;25(5):992–1008.
- [41] Schmidt T, Gaertner F, Kreye H. New developments in cold spray based on higher gas and particle temperatures. *J Therm Spray Techn.* 2006;15(4):488–494.
- [42] Qin WB, Li JS, Liu YY, et al. Effects of grain size on tensile property and fracture morphology of 316L stainless steel. *Mater Lett.* 2019;254:116–119.
- [43] Song J, Liu J, Chen Q, et al. Effect of the shape factor on the cold-spraying dynamic characteristics of sprayed particles. *J Therm Spray Techn.* 2017;26(8):1851–1858.
- [44] Samson T, MacDonald D, Fernández R, et al. Effect of pulsed waterjet surface preparation on the adhesion strength of cold gas dynamic sprayed aluminum coatings. *J Therm Spray Techn.* 2015;24(6):984–993.

- [45] Pattison J, Celotto S, Khan A, et al. Standoff distance and bow shock phenomena in the cold spray process. *Surf Coat Tech.* 2008;202(8):1443–1454.
- [46] Yin S, Wang X, Li W, et al. Numerical study on the effect of substrate angle on particle impact velocity and normal velocity component in cold gas dynamic spraying based on CFD. *J Therm Spray Techn.* 2010;19(6):1155–1162.
- [47] Binder K, Gottschalk J, Kollenda M, et al. Influence of impact angle and gas temperature on mechanical properties of titanium cold spray deposits. *J Therm Spray Techn.* 2010;20(1-2):234–242.
- [48] Gärtner F, Schmidt T, Stoltenhoff T, et al. Recent developments and potential applications of cold spraying. *Adv Eng Mater.* 2006;8(7):611–618.
- [49] Lee MW, Park JJ, Kim DY, et al. Numerical studies on the effects of stagnation pressure and temperature on supersonic flow characteristics in cold spray applications. *J Therm Spray Techn.* 2011;20(5):1085–1097.
- [50] Prisco U. Size-dependent distributions of particle velocity and temperature at impact in the cold-gas dynamic-spray process. *J Mater Process Tech.* 2015;216:302–314.
- [51] Yoon S, Kim HJ, Lee C. Deposition behavior of bulk amorphous NiTiZrSiSn according to the kinetic and thermal energy levels in the kinetic spraying process. *Surf Coat Tech.* 2006;200(20–21):6022–6029.
- [52] Meng X, Zhang J, Zhao J, et al. Influence of gas temperature on microstructure and properties of cold spray 304SS coating. *J Mater Sci Technol.* 2011;27(9):809–815.
- [53] Lioma D, Sacks N, Botef I. Cold gas dynamic spraying of WC–Ni cemented carbide coatings. *Int J Refract Met H.* 2015;49:365–373.
- [54] Qiao JH, Jin X, Qin JH, et al. A super-hard superhydrophobic Fe-based amorphous alloy coating. *Surf Coat Tech.* 2018;334:286–291.
- [55] Wang Y, Li MY, Sun LL, et al. Environmentally assisted fracture behavior of Fe-based amorphous coatings in chloride-containing solutions. *J Alloy Compd.* 2018;738:37–48.
- [56] Lin JR, Wang ZH, Cheng JB, et al. Effect of initial surface roughness on cavitation erosion resistance of arc-sprayed Fe-based amorphous/nanocrystalline coatings. *Coatings.* 2017;7(11):200.
- [57] Zhou H, Zhang C, Wang W, et al. Microstructure and mechanical properties of Fe-based amorphous composite coatings reinforced by stainless steel powders. *J of Mater Sci Technol.* 2015;31(1):43–47.
- [58] Gao M, Lu W, Yang B, et al. High corrosion and wear resistance of Al-based amorphous metallic coating synthesized by HVAF spraying. *J Alloy Compd.* 2018;735:1363–1373.
- [59] Shen Y, Perepezko JH. Al-based amorphous alloys: Glass-forming ability, crystallization behavior and effects of minor alloying additions. *J Alloy Compd.* 2017;707:3–11.
- [60] Goldman ME, Ünlü N, Shiflet GJ, et al. Selected corrosion properties of a novel amorphous Al-Co-Ce alloy system. *Electrochem Solid St.* 2005;8(2):B1, doi:10.1149/1.1848261.
- [61] Bahrami F, Amini R, Taghvaei AH. Microstructure and corrosion behavior of electrodeposited Ni-based nanocomposite coatings reinforced with Ni<sub>60</sub>Cr<sub>10</sub>Ta<sub>10</sub>P<sub>16</sub>B<sub>4</sub> metallic glass particles. *J Alloy Compd.* 2017;714:530–536.
- [62] Suresh K, Yugeswaran S, Rao KP, et al. Sliding wear behavior of gas tunnel type plasma sprayed Ni-based metallic glass composite coatings. *Vacuum.* 2013;88:114–117.
- [63] Wang D, Li P. Thermodynamic and mechanical properties of Cu–Zr–Al–Ti bulk metallic glasses. *AIP Adv.* 2018;8(12):125003.
- [64] Wang B, Xu KK, Shi XH, et al. Electrochemical and chemical corrosion behaviors of the in-situ Zr-based metallic glass matrix composites in chloride-containing solutions. *J Alloy Compd.* 2019;770:679–685.
- [65] Zhang Y, Yan L, Zhao X, et al. Enhanced chloride ion corrosion resistance of Zr-based bulk metallic glasses with cobalt substitution. *J Non-Cryst Solids.* 2018;496:18–23.
- [66] Wu J, Zhang SD, Sun WH, et al. Enhanced corrosion resistance in Fe-based amorphous coatings through eliminating Cr-depleted zones. *Corros Sci.* 2018;136:161–173.
- [67] Wang W, Zhang C, Zhang ZW, et al. Toughening Fe-based amorphous coatings by reinforcement of amorphous carbon. *Sci Rep-UK.* 2017;7(1):4084.
- [68] Tian WP, Yang HW, Zhang SD. Synergistic effect of Mo, W, Mn and Cr on the passivation behavior of a Fe-based amorphous alloy coating. *Acta Metall Sin-Engl.* 2017;31(3):308–320.
- [69] Jiao J, Luo Q, Wei X, et al. Influence of sealing treatment on the corrosion resistance of Fe-based amorphous coatings in HCl solution. *J Alloy Compd.* 2017;714:356–362.
- [70] Ajdelsztajn L, Jodoin B, Richer P, et al. Cold gas dynamic spraying of iron-base amorphous alloy. *J Therm Spray Techn.* 2006;15(4):495–500.
- [71] Guan L, Yan B, Long L, et al. Preliminary study of fabricating bulk Fe-based amorphous alloy by cold gas dynamic spraying. *Int J Mod Phys B.* 2009;23(6–7):1288–1293.
- [72] Henao J, Concustell A, Cano IG, et al. Influence of cold gas spray process conditions on the microstructure of Fe-based amorphous coatings. *J Alloy Compd.* 2015;622:995–999.
- [73] Yoon S, Kim J, Bae G, et al. Formation of coating and tribological behavior of kinetic sprayed Fe-based bulk metallic glass. *J Alloy Compd.* 2011;509(2):347–353.
- [74] Trexler MM, Thadhani NN. Mechanical properties of bulk metallic glasses. *Prog Mater Sci.* 2010;55(8):759–839.
- [75] Schuh C, Hufnagel T, Ramamurty U. Mechanical behavior of amorphous alloys. *Acta Mater.* 2007;55(12):4067–4109.
- [76] Qin WB, Liu YY, Yue W, et al. Influence of frictional interface state on tribological performance of sintered polycrystalline diamond sliding against different mating materials. *Tribol Lett.* 2019;67:87.
- [77] Choi SJ, Lee HS, Jang JW, et al. Corrosion behavior in a 3.5 wt% NaCl solution of amorphous coatings prepared through plasma-spray and cold-spray coating processes. *Met Mater Int.* 2014;20(6):1053–1057.
- [78] Sansoucy E, Kim GE, Moran AL, et al. Mechanical characteristics of Al-Co-Ce coatings produced by the cold spray process. *J Therm Spray Techn.* 2007;16(5-6):651–660.
- [79] Koh PK, Loke K, Yu SCM, et al. Deposition of amorphous aluminium powder using cold spray, Proceedings from the International Thermal Spray Conference and Exposition, Houston, Texas, USA, 2012.



- [80] Lahiri D, Gill PK, Scudino S, et al. Cold sprayed aluminum based glassy coating: Synthesis, wear and corrosion properties. *Surf Coat Tech.* **2013**;232:33–40.
- [81] Henao J, Concustell A, Cano IG, et al. Novel Al-based metallic glass coatings by cold gas spray. *Mater Design.* **2016**;94:253–261.
- [82] Choi H, Yoon S, Kim G, et al. Phase evolutions of bulk amorphous NiTiZrSiSn feedstock during thermal and kinetic spraying processes. *Scripta Mater.* **2005**;53(1):125–130.
- [83] Yoon S, Lee C, Choi H, et al. Evaluation of the effects of the crystallinity of kinetically sprayed Ni–Ti–Zr–Si–Sn bulk metallic glass on the scratch response. *Mat Sci Eng A.* **2007**;449–451:285–289.
- [84] Choi H, Jo H, An K, et al. Tribological behavior of the kinetic sprayed Ni<sub>59</sub>Ti<sub>16</sub>Zr<sub>20</sub>Si<sub>2</sub>Sn<sub>3</sub> bulk metallic glass. *J Alloy Compd.* **2007**;434–435:64–67.
- [85] Wang AP, Chang XC, Hou WL, et al. Preparation and corrosion behaviour of amorphous Ni-based alloy coatings. *Mat Sci Eng A.* **2007**;7449–451:277–280.
- [86] List A, Gärtner F, Mori T, et al. Cold spraying of amorphous Cu<sub>50</sub>Zr<sub>50</sub> Alloys. *J Therm Spray Techn.* **2015**;24(1–2):108–118.
- [87] El-Eskandrany MS, Al-Azmi A, et al. Potential applications of cold sprayed Cu<sub>50</sub>Ti<sub>20</sub>Ni<sub>30</sub> metallic glassy alloy powders for antibacterial protective coating in medical and food sectors. *J Mech Behav Biomed.* **2016**;56:183–194.
- [88] Liu L, Qiu CL, Huang CY, et al. Biocompatibility of Ni-free Zr-based bulk metallic glasses. *Intermetallics.* **2009**;17(4):235–240.
- [89] Sun YS, Zhang W, Kai W, et al. Evaluation of Ni-free Zr–Cu–Fe–Al bulk metallic glass for biomedical implant applications. *J Alloy Compd.* **2014**;586: S539–S543.
- [90] Kwon DH, Park ES, Huh MY, et al. Wear behavior of Fe-based bulk metallic glass composites. *J Alloy Compd.* **2011**;509:S105–S108.
- [91] Wang Y, Shi L, Duan D, et al. Tribological properties of Zr<sub>61</sub>Ti<sub>2</sub>Cu<sub>25</sub>Al<sub>12</sub> bulk metallic glass under simulated physiological conditions. *Mat Sci Eng C.* **2014**;37:292–304.
- [92] Kang N, Coddet P, Liao H, et al. The effect of heat treatment on microstructure and tensile properties of cold spray Zr base metal glass/Cu composite. *Surf Coat Tech.* **2015**;280:64–71.